

MedChemComm

Accepted Manuscript



This is an *Accepted Manuscript*, which has been through the Royal Society of Chemistry peer review process and has been accepted for publication.

Accepted Manuscripts are published online shortly after acceptance, before technical editing, formatting and proof reading. Using this free service, authors can make their results available to the community, in citable form, before we publish the edited article. We will replace this *Accepted Manuscript* with the edited and formatted *Advance Article* as soon as it is available.

You can find more information about *Accepted Manuscripts* in the [Information for Authors](#).

Please note that technical editing may introduce minor changes to the text and/or graphics, which may alter content. The journal's standard [Terms & Conditions](#) and the [Ethical guidelines](#) still apply. In no event shall the Royal Society of Chemistry be held responsible for any errors or omissions in this *Accepted Manuscript* or any consequences arising from the use of any information it contains.

Cite this: DOI: 10.1039/c0xx00000x

www.rsc.org/xxxxxxx

ARTICLE TYPE

Discovery of Dehydroabietylamine Derivatives as Multifunctional Agents for the Treatment of Alzheimer's Disease

Yingying Cao^{a,†}, Ling Wang^{a,†}, Zhongxiang Lin^b, Fengyin Liang^c, Zhong Pei^c, Jun Xu^a, Qiong Gu^{a,*}

Received (in XXX, XXX) Xth XXXXXXXXXX 20XX, Accepted Xth XXXXXXXXXX 20XX

DOI: 10.1039/b000000x

Dehydroabietylamine derivatives have been reported to eliminate the superoxide anion ($O_2^{\cdot-}$) and 1,1-diphenyl-2-picrylhydrazyl (DPPH) radicals. Herein, several dehydroabietylamine derivatives showed potent anti-oxidative activity in SH-SY5Y cells and exhibited significant inhibition of A β 2 self-mediated aggregation and the disaggregation of A β 2 aging fibrils. In particular, compound 12N, 18N-bis(caffeoyl)-14-nitrodehydroabietylamine (**3b**) showed the most potent inhibition activity against A β 2 self-mediated aggregation with an IC₅₀ value of 3.96±0.33 μ M. Moreover, compound **3b** decreased the production of A β 2 in swAPP HEK293 cells and showed neuroprotective activity against A β 2-induced cytotoxicity. Furthermore, through reducing the production of A β 2 species, compound **3b** alleviated A β 2-induced paralysis in transgenic *Caenorhabditis elegans* strain CL4176. Considering its multifunctional activity and lower cytotoxicity, **3b** is considered a potential multifunctional agent for the treatment of Alzheimer's disease.

Introduction

Alzheimer's disease (AD) is a progressive neurodegenerative disorder characterized by cognitive impairment and memory loss^{1,2}. It has been reported that AD is caused and proceeded by many factors, such as oxidative stress, β -amyloid (A β) and τ -protein formation, neuronal toxicity, and acetylcholine breakdown³. The brains of AD patients feature characteristic A β plaques; therefore, great attention has been paid to this 39-43 residue polypeptide, which is derived from the hydrolysis of amyloid precursor protein (APP)⁴⁻⁶. Serious neuronal toxicity may arise from the aggregation and deposition of A β species in the brain as oligomers or fibrils⁷. Consequently, reducing the production and aggregation of A β has been considered an important approach for the treatment of AD. Several natural products have also been reported to reduce the production of A β , such as curcumin (Cur)⁸ and berberine⁹. Animal experiments have proven that polyphenols show neuroprotective effects on A β -induced toxicity as well¹⁰⁻¹². In addition, oxidative damage also plays an important role in this neurodegenerative disease^{13, 14}. One of the earliest pathological features in AD pathogenesis is oxidative stress. Agents with anti-oxidative ability may also have potent anti-amyloid aggregation activity, as elucidated by the polyphenols¹⁵. Therefore, multifunctional compounds for the treatment of AD are desirable¹⁶. Finding multi-targeted agents with anti-oxidant and A β inhibitory activity as well as the ability to reduce oxidative stress, A β self-mediated aggregation, and A β -induced neurocytotoxicity might be an effective therapeutic strategy for AD¹⁷⁻²¹.

Dehydroabietylamine, which contains a phenanthrene ring structure, is the main component of rosin amine and has been

comprehensively studied for its wide range of biological effects. Dehydroabietylamine derivatives show anti-microbial, anti-viral, anti-inflammatory, and free radical scavenging activity²²⁻²⁵. In the previous study, we synthesized and evaluated the anti-oxidant activity of the dehydroabietylamine derivatives *in vitro*²⁶. Here, a series of dehydroabietylamine derivatives (Table 1) were evaluated for the treatment of AD, which included examining their anti-oxidative activity in SH-SY5Y cells, their inhibition of A β aggregation, and their neuroprotective effect. Furthermore, the activity of 12N, 18N - bis (caffeoyl) - 14 - nitrodehydroabietylamine (**3b**) was sufficiently studied using Thioflavin T (ThT)²⁷, circular dichroism (CD) spectra^{28, 29}, transmission electron microscopy (TEM), and molecular dynamics (MD) simulations. Moreover, swAPP HEK293 cells transfected with APP695³⁰ and *Caenorhabditis elegans* strain CL4176 were also used to evaluate their ability to inhibit the production of A β and alleviate the paralysis process of *C. elegans*³¹.

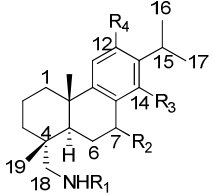
Results and discussion

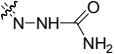
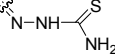
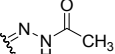
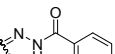
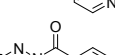
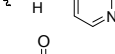
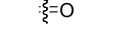
In the previous study, we have reported the design and synthesis of 22 dehydroabietylamine derivatives with their anti-oxidant activities *in vitro*²⁶. Herein, their anti-oxidant activities were evaluated by the levels of ROS generation in SH-SY5Y cell lines³². Most compounds didn't show cytotoxicities at the tested concentration of 10 μ M. Curcumin (Cur) was used as a positive control. Compared with Cur, eight compounds (**1a**, **1b**, **1c**, **2j**, **3b**, **3c**, **3d**, and **3e**) significantly reduced the generation of ROS in SH-SY5Y cells (Table 1). These results indicated that eight compounds showed better anti-oxidant activity than Cur.

Cite this: DOI: 10.1039/c0xx00000x

www.rsc.org/xxxxxx

ARTICLE TYPE

Table 1 The structures of 22 compounds and their activities at anti-oxidant and against A β aggregation


Comps	R ₁	R ₂	R ₃	R ₄	^a ROS	^b A β aggregation inhibition	^c β aging fibrils disaggregation
1	H	H	H	H	N/A	N/A	N/A
1a		H	H	H	50.84 \pm 3.25	74.63 \pm 1.28	48.98 \pm 1.48
1b		H	H	H	41.75 \pm 4.98	55.26 \pm 1.35	37.63 \pm 1.30
1c		H	H	H	48.23 \pm 2.19	20.57 \pm 1.98	8.93 \pm 3.24
1d		H	H	H	26.06 \pm 2.54	24.53 \pm 2.31	10.72 \pm 1.21
2	H		H	H	N/A	N/A	N/A
2a			H	H	13.35 \pm 1.24	N/A	N/A
2b			H	H	N/A	N/A	N/A
2c			H	H	N/A	N/A	N/A
2d			H	H	N/A	N/A	N/A
2e			H	H	N/A	N/A	N/A
2f			H	H	10.4 \pm 3.27	N/A	N/A
2g			H	H	34.14 \pm 1.09	N/A	N/A
2h			H	H	19.77 \pm 2.45	N/A	N/A
2i			H	H	N/A	N/A	N/A
2j			H	H	41.18 \pm 2.01	N/A	N/A
3	H	H	NO ₂	NH ₂	N/A	N/A	N/A
3a		H	NO ₂	NH ₂	31.24 \pm 2.18	26.07 \pm 2.15	14.25 \pm 3.72

3b		H	NO ₂		62.44±4.58	91.95±1.45	82.78 ± 1.37
3c		H			53.85±5.13	93.3 ±2.39	82.46 ± 2.04
3d		H	NO ₂		42.19±4.32	72.97±2.78	48.92 ± 3.03
3e		H	NO ₂		48.4±4.35	77.87±2.46	51.99 ± 1.29
Cur	N/A	N/A	N/A	N/A	37.87±2.35	70.6 ±1.89	48.74 ± 1.34

^a **ROS**: was measured using DCFH-DA in SH-SY5Y cells after incubation with or without 10 μM of the dehydroabietylamine derivatives or Cur (positive control). The results are described as the inhibition rate. The mean±the SD value is the expression of at least four independent measurements. ^b ThT fluorescence assay was used to detect aggregated Aβ₄₂ by microplate reader at 450 nm and 490 nm. The inhibition rate of Aβ₄₂ aggregation by dehydroabietylamine and its derivatives as well as Cur (Cur) at 50 μM compared with the negative control. ^c The disaggregation rate of Aβ₄₂ preformed fibrils by the dehydroabietylamine derivatives and Cur at 50 μM by the ThT assays.

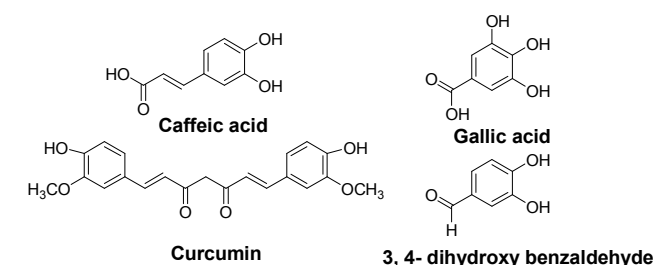


Fig.1 Structures of caffeic acid, gallic acid, 3,4-dihydroxybenzaldehyde, and curcumin (Cur).

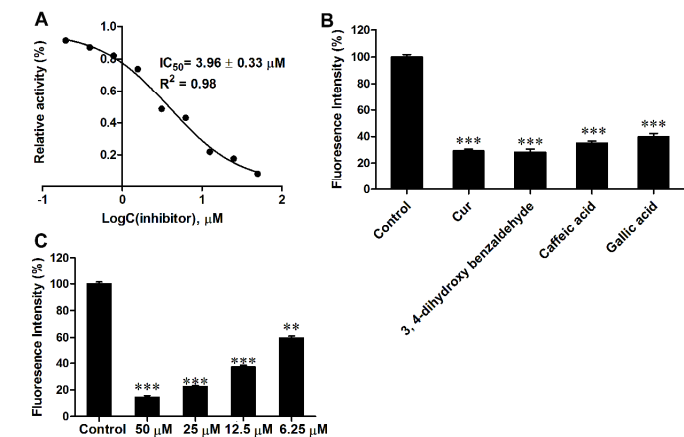


Fig.2 Compound **3b**, caffeic acid, gallic acid, 3,4-dihydroxybenzaldehyde, and curcumin (Cur) inhibit Aβ₄₂ aggregation and **3b** disaggregates preformed fibrils. (A) The IC₅₀ of **3b** against Aβ₄₂ aggregation; (B) The inhibition rate against Aβ₄₂ aggregation by caffeic acid, gallic acid, 3,4-dihydroxybenzaldehyde, and Cur at 50 μM; (C) The effect of **3b** on the disaggregation of Aβ₄₂ preformed fibrils at varying concentrations. Data represent the mean±the SEM from 5 independent experiments. ***P<0.001 and **P<0.01 compared to untreated control samples.

The Thioflavin T (ThT) fluorescence method was used to measure the inhibitory activities of compounds against Aβ₄₂ self-mediated aggregation and the disaggregation of Aβ₄₂ aging fibrils. Cur was used as the reference compound and the results are summarized in Table 1. According to the results, most compounds (**1a**, **1b**, **1c**, **1d**, **3a**, **3b**, **3c**, **3d**, and **3e**) showed

moderate to potent inhibition activity (20.6% to 92.0%) compared with Cur (70.6%) at 50 μM. Moreover, six compounds **1a**, **1b**, **3b**, **3c**, **3d**, and **3e** also disaggregated the Aβ₄₂ aging fibrils. Furthermore, the inhibitory activities of these compounds are similar to the trend of their anti-oxidant activities in SH-SY5Y cells. Noticeably, compound **3b** showed the most potent activity against Aβ₄₂ aggregation with an IC₅₀ value of 3.96±0.33 μM (Fig. 2A). As shown in Fig. 2C, compound **3b** also disaggregated the Aβ₄₂ aging fibrils in a dose-dependent manner. In addition, the inhibitory activities of the substitute moieties (caffeic acid, gallic acid, and 3,4-dihydroxybenzaldehyde) at 50 μM were also evaluated (Fig. 2B). As shown in Table 1, the dehydroabietylamine scaffold (**1**) and the substitute moieties (caffeic acid, gallic acid, and 3,4-dihydroxybenzaldehyde) did not display good inhibitory activity. While the inhibition activity increased when the substituent was positioned at C-18, which indicated that this substituent is necessary for their inhibition activities. The dehydroabietylamine derivative with the caffeic acetyl substituent (**3b**) showed higher activity than the 3,4-dihydroxyl benzoyl substituted compound (**3a**). Furthermore, the compounds with two caffeic acetyls substituted at C-18 and C-12 exhibited better activity than one benzoyl substituted at C-18. However, three caffeic acetyl moieties substituted at C-12, C-14, and C-18 (**3c**) decreased the activity. These results indicated that the caffeic acid, gallic acid, and 3,4-dihydroxybenzaldehyde fragments can increase the inhibitory effect of dehydroabietylamine.

CD spectroscopy was used to measure the transition structure of Aβ₄₂, which includes α-helices, β-sheets, and random coils in the process of self-mediated aggregation and fibrillation. The β-sheet conformation was considered important in Aβ₄₂ aggregation. The CD spectra of α-helices and β-sheets occur at approximately 217 and 195 nm, respectively. As shown in Fig. 3, after 48 h of incubation, 40 μM **3b** reduced the formation β-sheet structures and increased the formation of α-helices. Therefore, it was suggested that **3b** could inhibit the formation of β-sheets.

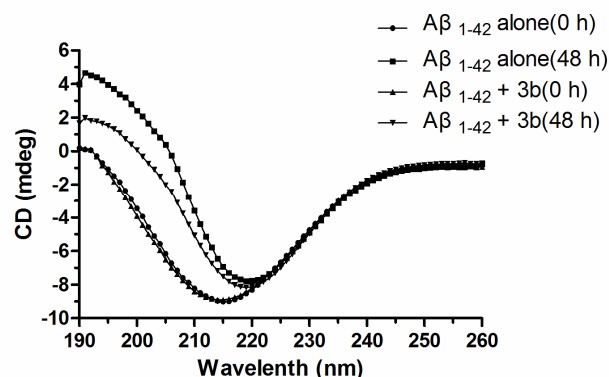


Fig. 3 CD spectra of the $A\beta_{42}$ secondary structure with and without **3b**. The CD spectra at 0 and 48 h were recorded using a wavelength range of 190–260 nm. The concentration of $A\beta_{42}$ in 20 mM PBS was 20 μM and **3b** was present at 40 μM .

To further study the ability of compound **3b** to inhibit $A\beta_{42}$ aggregation, TEM studies were performed (Fig. 4). Fresh $A\beta_{42}$ (25 μM) was incubated untreated or with 50 μM **3b** at 37 $^{\circ}\text{C}$ for 48 h. Many fibrils were observed (Fig. 4A) when the $A\beta_{42}$ peptide was incubated alone, while few fibrils were observed (Fig. 4B) when $A\beta_{42}$ was incubated with 50 μM **3b**. These results suggested that **3b** could significantly inhibit the formation of amyloid fibrils. In addition, after 25 μM aggregated $A\beta_{42}$ peptide was incubated in the absence or presence of 50 μM **3b** for another 48 h at 37 $^{\circ}\text{C}$, amorphous aggregations were extensively observed (Fig. 4D) when no **3b** was present, but many short fibrils as balls were observed in the presence of **3b** (Fig. 4C). Therefore, based on the TEM and ThT assay results, we can conclude that compound **3b** effectively inhibits $A\beta_{42}$ fibril formation and disaggregates the $A\beta_{42}$ aging fibrils.

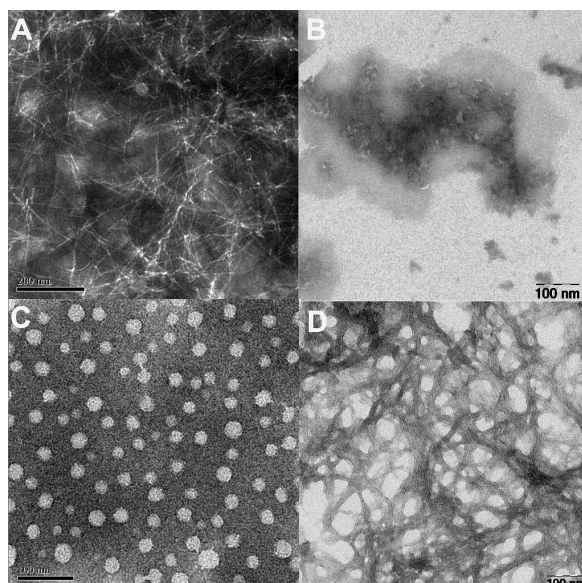


Fig. 4 TEM image analysis of the aggregation of 25 μM $A\beta_{42}$ and the disaggregation of preformed fibrils in the absence or presence of 50 μM **3b**. $A\beta_{42}$ (25 μM) with (B) and without (A) 50 μM **3b**. The fibrils were incubated for 48 h at 37 $^{\circ}\text{C}$, and then incubated with preformed $A\beta_{42}$ fibrils for another 48 h with 20 mM PBS (D) or 50 μM **3b** (C).

To explore the binding mode of **3b** and $A\beta_{42}$, molecular

docking and molecular dynamics (MD) studies were performed. The crystal structure of $A\beta_{42}$ used in the docking study was obtained from the Protein Data Bank (1IYT). As shown in Fig. 5A, **3b** is bound to the C-terminus of $A\beta_{42}$ and forms a hydrogen bond with Ala30. After 90 ns MD simulations in water, the representation conformation of **3b** and $A\beta_{42}$ was calculated based on clustering analysis and is described in Fig. 5B. MD results indicated that **3b** interacts primarily through hydrophobic interactions with $A\beta_{42}$, and forms two hydrogen bonds with Ala30 and Gly9. The RMSD evolution curves (Fig. 5C) indicated that the complex of $A\beta_{42}$ and **3b** became stable after 19 ns. The time evolution of the secondary structures changes of $A\beta_{42}$ in the complex of $A\beta_{42}$ and **3b** was calculated and showed in Fig. 5D. Fig. 5D showed that most residues (2–15, 32–35) adopted α -helical structure; residues 15–23 formed α -helix or 3-helix; residues 35–42 mainly adopted coil and bend structure at the C-terminus of $A\beta_{42}$, while residues 23–32 mainly formed turn structure (occasionally, bend and 3-helix). β -sheet structure is not observed during the whole 90 ns simulation in water. These results indicated **3b** can stabilize α -helices and further inhibit the conversion of many secondary structures into β -sheets. MD results are consistent with our CD experimental results. Therefore, it can be concluded that **3b** inhibits $A\beta_{42}$ aggregation by stabilizing the α -helix structure.

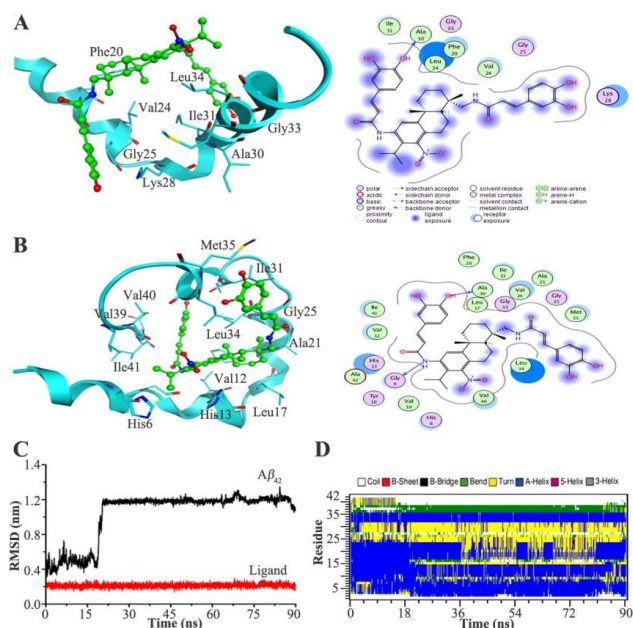


Fig. 5 The binding mode of **3b** and $A\beta_{42}$. (A) **3b** was docked into the C-terminus of the α -helical conformation of $A\beta_{42}$. (B) The binding mode of **3b** and $A\beta_{42}$ was calculated from simulations. Hydrogen bonds are represented by blue lines. (C) The black line represents the RMSD of the $A\beta$ helix for $A\beta_{42}$ (black) and the red line represents the **3b**- $A\beta_{42}$ complex compared to their previous conformational changes over time. (D) The time evolution of the secondary structures of $A\beta_{42}$ in the presence of **3b**.

To further evaluate the cell viability and the neuroprotective effect of the dehydroabietylamine derivatives, MTT assay was used on the human neuroblastoma cell line SH-SY5Y. The compounds that inhibited $A\beta_{42}$ aggregation (**1a**, **1b**, **1c**, **1d**, **3b**, **3c**, **3d**, and **3e**) were chosen to evaluate their cell viability. As indicated in Fig. 6A, except for **3e**, compounds **1a**, **1b**, **1c**, **1d**, **3b**, **3c**, and **3d** at 10 μM did not affect cell viability. Especially,

compound **3b** did not show significant effect on cell viability in the concentration range of 1-50 μM (Fig. 6C). Moreover, the IC_{50} value of **3b** for the inhibition of $\text{A}\beta_{42}$ aggregation was below 10 μM , which showed promise for future applications. The activity of **3b** on $\text{A}\beta_{42}$ -induced cytotoxicity was also measured. As shown in Fig. 6B, after incubation at 37 $^{\circ}\text{C}$ for 48 h, 20 μM $\text{A}\beta_{42}$ oligomers caused a significant decrease in the cell viability rate to

50.02 \pm 4.98% of the control ($P < 0.001$), while the co-incubation of 20 μM $\text{A}\beta_{42}$ with varying concentrations of **3b** (5, 10, 25, and 50 μM) increased the cell viability rate from 53.5% to 74.04%. Therefore, **3b** could reduce the $\text{A}\beta_{42}$ -induced cytotoxicity in the SH-SY5Y cell line, which indicated that **3b** could be considered a neuroprotective agent for the treatment of AD.

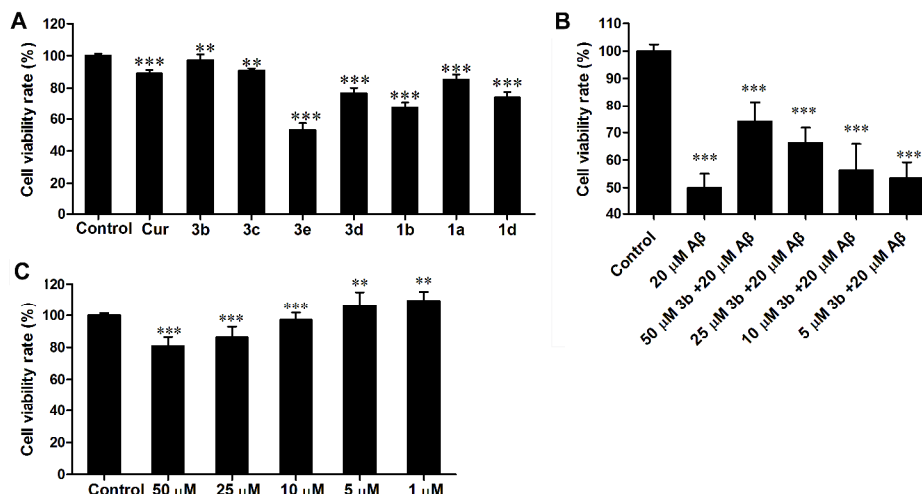


Fig. 6 Cell viability in the absence or presence of dehydroabietylamine derivatives, and the neuroprotective effect of **3b** at various concentrations on $\text{A}\beta_{42}$ -induced cytotoxicity (20 μM). (A) Dehydroabietylamine derivatives (10 μM) were added to SH-SY5Y cells for 48 h and then the cell viability was determined. (B) Pre-incubated mixtures of $\text{A}\beta_{42}$ (20 μM) left untreated or treated with various concentrations of **3b** for 48 h. The cell viability was measured using the MTT method and the data are represented as the mean \pm the SD of four independent experiments. The significant neuroprotective activity of **3b** was observed in a dose-dependent manner at all tested concentrations (***) $P < 0.001$, **) $P < 0.01$. (C) **3b** (50, 25, 10, 5, and 1 μM) was added to SH-SY5Y cells for 48 h. The compound-free (untreated) cells were considered the negative control.

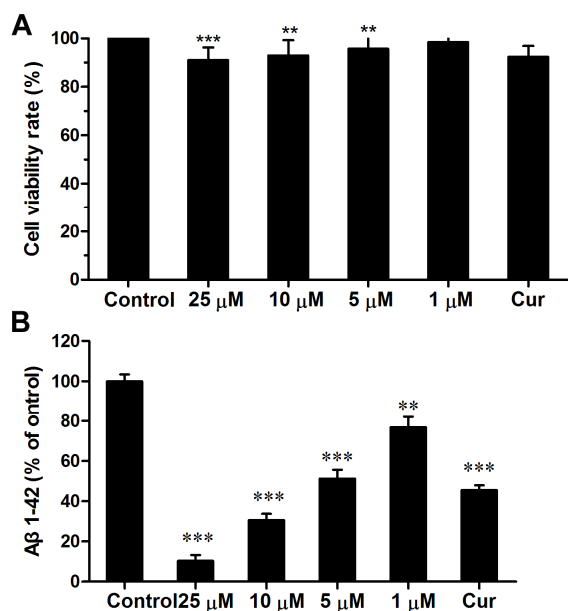


Fig. 7 Inhibition of the production of $\text{A}\beta_{42}$ in HEK293 cells by **3b** as measured by ELISA assay. (A) The effect of **3b** (25, 10, 5, and 1 μM) on the cytotoxicity of HEK293 cells incubated at 37 $^{\circ}\text{C}$ for 48 h, where Cur (10 μM) was used as the positive control. (***) $P < 0.001$, **) $P < 0.01$, and $P > 0.05$ compared with untreated cells ($n=5$). (B) The effect of varied concentrations of **3b** (25, 10, 5, and 1 μM) on the production of $\text{A}\beta_{42}$ after incubation for 48 h. (***) $P < 0.001$ and **) $P < 0.01$ compared with the vehicle-treated group ($n=5$).

In order to test the effect of **3b** on the production of $\text{A}\beta_{42}$ in the cell level, swAPP HEK293 cell lines were used. First, the cell viability of swAPP HEK293 cells treated with **3b** was measured using the MTT method. As shown in Fig. 7A, the cell viability did not decline significantly when treated with **3b** at 25, 10, 5, and 1 μM . Moreover, compared with the control group, the cell viability rate was above 90% at 25 μM **3b**. A sandwich ELISA assay was used to detect extracellular $\text{A}\beta_{42}$ levels in the conditioned media from HEK293 cells. As shown in Fig. 7B, after 48 h of incubation, 25 μM **3b** remarkably reduced the extracellular $\text{A}\beta_{42}$ levels of the control (100 \pm 3.45%) to 10.4 \pm 2.89% ($n=4$; $P < 0.001$). Cur was used as a reference, which reduced the extracellular $\text{A}\beta_{42}$ levels of the control from 100 \pm 3.45% to 45.6 \pm 2.38% ($n=4$; $P < 0.001$) at 10 μM . According to these results, **3b** may be regarded as a potential agent for the treatment of AD by reducing the production of $\text{A}\beta_{42}$.

To determine whether **3b** could reduce $\text{A}\beta$ -induced toxicity *in vivo*, a transgenic *C. elegans* model was used that highly expresses the $\text{A}\beta$ peptide, which can lead to paralysis. After synchronization for 12 h, the transgenic worms were placed on OP50 food containing 0.1% DMSO or **3b** (10, 50, 200, and 500 μM) at 15 $^{\circ}\text{C}$ for 12 h. The worms were then transferred to 26 $^{\circ}\text{C}$ to induce $\text{A}\beta$ expression for an additional 36 h. Huperzine A (Hup A, 500 μM) was used as a positive control. The worms were regarded as paralyzed when they were touched with a platinum loop and didn't move. Fig. 8A showed the time course of the paralysis rate of *C. elegans* CL4176 worms fed with vehicle (0.1% DMSO; filled circles), Hup A (500 μM ; filled circles) and **3b** (10, 50, 200, and 500 μM ; filled circles) after the 36 h

30

induction of A β expression. A delay of paralysis by **3b** at 10 and 50 μ M was observed in comparison with the control group. Moreover, 50 μ M **3b** was better than 500 μ M Hup A in delaying A β -induced paralysis. Fig. 8C is a set of histograms representing the average life expectancy of untreated CL4176 worms or worms treated with **3b**. According to these data, the average life expectancy of CL4176 worms was 46.9 ± 0.54 h (n=4; P<0.001) when they were cultured with OP50 alone; however, **3b** extended the average life expectancy of CL4176 to 48.2 ± 0.55 h (n=4; P<0.001) at 10 μ M and 50.5 ± 0.55 h (n=4; P<0.001) at 50 μ M (n=4; P<0.001). Moreover, **3b** had more activity than 500 μ M Huperzine A, which could extend the average life expectancy of CL4176 to 48.3 ± 0.12 h (n=4; P<0.001). However, 200 and 500

μ M **3b** did not extend the average life expectancy of CL4176; in fact, it reduced it to 45.8 ± 0.58 h (n=4; P<0.01) and 44.7 ± 0.34 h (n=4; P<0.001), respectively. This suggested that high concentrations of **3b** may be toxic for the CL4176 worms and speeded up A β -induced paralysis.

To detect whether **3b** can reduce the expression of A β species in *C. elegans* strain CL4176, western blot assays were used to measure the levels of A β species in CL4176. As shown in Fig. 8B and 8D, **3b** (10 and 50 μ M) reduced the expression of A β species in the control from 1.00 ± 0.03 (n=4) to 0.71 ± 0.05 (n=4; P<0.001) and 0.45 ± 0.07 (n=4; P<0.001), respectively. These results suggested that **3b** can reduce the expression of A β species and delay A β -induced toxicity in *C. elegans* strain CL4176.

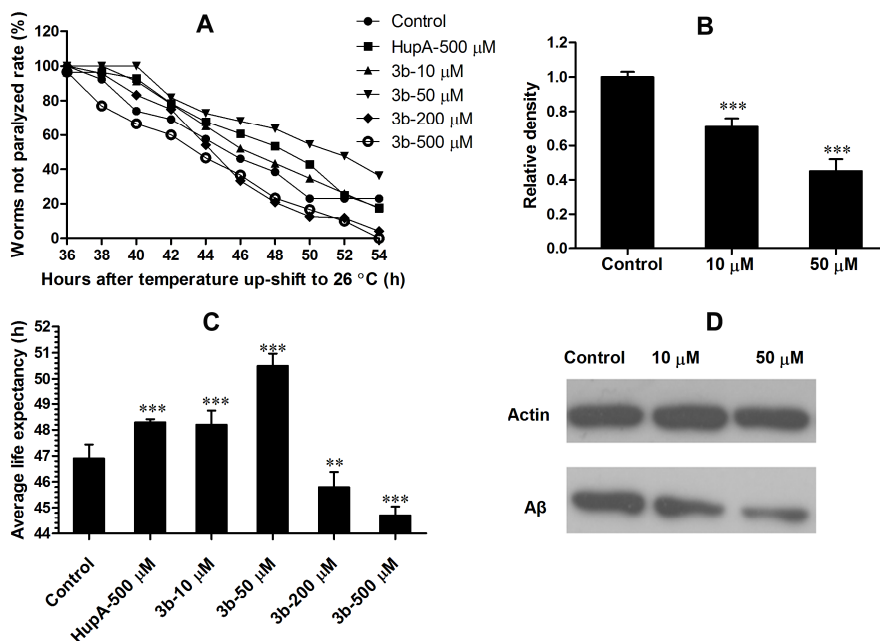


Fig. 8 Effect of **3b** on A β -induced paralysis in *Caenorhabditis elegans* CL4176. (A) Time course of the paralysis assays in CL4176 worms fed with or without different concentrations of **3b**. Huperzine A (500 μ M) was used as a positive control. (B) A representative western blot of the expression of the A β species in transgenic *C. elegans* CL4176 worms fed vehicle or **3b** (10 and 50 μ M). The worms were maintained and scored at 26 $^{\circ}$ C. When the non-paralyzed worms constituted 50% of all worms, they were collected, loaded on gel lane (80 μ g) and immunoblotted with the 6E10 antibody. (C) The average life expectancy of CL4176 worms fed vehicle or **3b**. Vehicle (control), Huperzine A (Hup A, 500 μ M), or **3b** (10, 50, 200 and 500 μ M) was added into the 35 \times 10 mm culture plates, maintained at 16 $^{\circ}$ C for 48 h and then shifted to 26 $^{\circ}$ C to induce the expression of A β . The paralysis was recorded at 2 h intervals. The results are expressed as the percentage of non-paralyzed worms from at least four independent assays of 50 worms per experiment. (D) The quantification of immunoreactive A β species by Western blot. The results are expressed as the relative density of the previously indicated band from four independent experiments. ***P<0.001 compared with the vehicle-treated group (n=4).

Conclusions

In summary, eight dehydroabietylamine derivatives (**1a**, **1b**, **1c**, **2j**, **3b**, **3c**, **3d**, and **3e**) showed anti-oxidant activity in the SH-SY5Y cell line, and six (**1a**, **1b**, **3b**, **3c**, **3d**, and **3e**) of these simultaneously displayed a potent inhibitory effect on A β ₄₂ aggregation and the disaggregation of A β ₄₂ aging fibrils. In particular, **3b** exhibited the most potent activity compared to the control of Cur. SAR analysis suggested that the introduction of two aromatic structure linkers at the C-18 and C-2 position of dehydroabietylamine is crucial for the inhibition of A β ₄₂ aggregation. The CD and MD assays indicated that **3b** reduced the formation of β -sheets and stabilized α -helices. The TEM experiment further showed that **3b** not only inhibited A β ₄₂

aggregation and fibril formation but also disaggregated the aging fibrils. Moreover, **3b** showed low cell toxicity in SH-SY5Y and swAPP HEK293 cells, and exhibited a protective effect on the A β ₄₂-induced neurotoxicity. Besides that, compound **3b** also reduced the secretion of extracellular A β ₄₂ in the swAPP HEK293 cells. Furthermore, **3b** delayed A β ₄₂-induced paralysis in *C. elegans* strain CL4176 and reduced the expression of A β ₄₂ species in CL4176. Therefore, **3b** exhibited multifunctional activity for the treatment of AD. These evidence provided important information to support the structure optimization of **3b** and to develop dehydroabietylamine derivatives as multifunctional agents for AD treatment.

Acknowledgments

This work was funded in part of the National Natural Science Foundation of China (No. 81001372, 81173470, 31170536), the National High-tech R&D Program of China (863 Program) (2012AA020307), and the introduction of innovative R&D team program of Guangdong Province (NO. [2009010058](#)). Some strains were provided by the CGC, which was funded by NIG Office of Research Infrastructure Programs (P40 OD010440).

Notes and references

^a School of Pharmaceutical Sciences, Sun Yat-Sen University, 132 East Circle Road at University City, Guangzhou, 510006, China

^b College of Chemical Engineering Nanjing Forestry University, Nanjing 210037, China

^c Neurology Department of the First Affiliated Hospital, Sun Yat-Sen University, Guangzhou 510080, China

¹⁵ Electronic Supplementary Information (ESI) available: [details of experimental procedures, materials and methods]. See DOI: 10.1039/b000000x/

[†] Equal contribution

*Correspondence to: guqiong@mail.sysu.edu.cn, Tel: +86-20-3994-3077
²⁰ Fax: +86-20-3994-3077

Reference

- 1 R. Brookmeyer, E. Johnson, K. Ziegler-Graham, H. M. Arrighi. *Alzheimer's & dementia*, 2007, **3**, 186-191.
- ²⁵ 2 B. Reisberg, R. Doody, A. Stöffler, F. Schmitt, S. Ferris, H. J. Möbius. *New England Journal of Medicine*, 2003, **14**, 1333-1341.
- 3 E. Bossy-Wetzel, R. Schwarzenbacher, S. A. Lipton. *Nat Med*, 2004, **S2-9**.
- 4 S. Barghorn, V. Nimmrich, A. Striebing, C. Krantz, P. Keller, B. Janson, M. Bahr, M. Schmidt, R. S. Bitner, J. Harlan. *Journal of neurochemistry*, 2005, **3**, 834-847.
- 5 I. Hamley. *Chemical Reviews*, 2012, **10**, 5147-5192.
- 6 J. Hardy, D. J. Selkoe. *Science*, 2002, **5580**, 353-356.
- 7 L.-F. Lue, Y.-M. Kuo, A. E. Roher, L. Brachova, Y. Shen, L. Sue, T. Beach, J. H. Kurth, R. E. Rydel, J. Rogers. *The American journal of pathology*, 1999, **3**, 853-862.
- ³⁵ 8 C. Zhang, A. Browne, D. Child, R. E. Tanzi. *J Biol Chem*, 2010, **37**, 28472-28480.
- 9 M. D. da Rocha, F. P. Viegas, H. C. Campos, P. C. Nicastro, P. C. Fossaluzza, C. A. Fraga, E. J. Barreiro, C. Viegas, Jr., *CNS Neurol Disord Drug Targets*, 2011, **2**, 251-270.
- ⁴⁰ 10 A. S. Darvesh, R. T. Carroll, A. Bishayee, W. J. Geldenhuys, C. J. Van der Schyf. *Expert review of neurotherapeutics*, 2010, **5**, 729-745.
- 11 P.-N. Cheng, C. Liu, M. Zhao, D. Eisenberg, J. S. Nowick. 2012.
- ⁴⁵ 12 M. Pappolla, R. Reiter, T. Bryant-Thomas, B. Poeggeler. *Current Medicinal Chemistry-Immunology, Endocrine & Metabolic Agents*, 2003, **1**, 33-46.
- 13 Y. Y. Cao, L. Wang, H. Ge, X. L. Lu, Z. Pei, Q. Gu, J. Xu. *Molecular Diversity*, 2013, **3**, 515-524.
- ⁵⁰ 14 P. Somporn, C. Phisalaphong, S. Nakornchai, S. Unchern, N. P. Morales. *Biological and Pharmaceutical Bulletin*, 2007, **1**, 74-78.
- 15 S. Bastianetto, S. Krantic, R. Quirion. *Mini reviews in medicinal chemistry*, 2008, **5**, 429-435.
- 16 A. Thapa, E.-R. Woo, E. Y. Chi, M. G. Sharoar, H.-G. Jin, S. Y. Shin, I.-S. Park. *Biochemistry*, 2011, **13**, 2445-2455.
- ⁵⁵ 17 Y. Cao, L. Wang, H. Ge, X. Lu, Z. Pei, Q. Gu, J. Xu. *Molecular Diversity*, 2013, **3**, 515-524.
- 18 Y.-P. Chen, Z.-Y. Zhang, Y.-P. Li, D. Li, S.-L. Huang, L.-Q. Gu, J. Xu, Z.-S. Huang. *European Journal of Medicinal Chemistry*, 2013.
- ⁶⁰ 19 H. He, X. Li, H. D. Wang, W. T. Zhang, H. Y. Jiang, S. J. Wang, L. H. Yuan, Y. Liu, X. Q. Liu. *Journal of Cardiovascular Pharmacology*, 2013, **6**, 482-488.
- 20 L. Huang, C. Lu, Y. Sun, F. Mao, Z. Luo, T. Su, H. Jiang, W. Shan, X. Li. *Journal of Medicinal Chemistry*, 2012, **19**, 8483-8492.
- ⁶⁵ 21 F. Mao, L. Huang, Z. Luo, A. Liu, C. Lu, Z. Xie, X. Li. *Bioorganic & medicinal chemistry*, 2012.

- 22 X. Rao, Z. Song, L. He. *Heteroatom Chemistry*, 2008, **5**, 512-516.
- 23 W. W. Wilkerson, W. Galbraith, I. DeLuca, R. R. Harris. *Bioorganic & Medicinal Chemistry Letters*, 1993, **10**, 2087-2092.
- ⁷⁰ 24 R. Xiaoping, S. Zhanqian, G. Hong. *CHEMISTRY-PEKING-*, 2006, **3**, 168.
- 25 S. ZHANG, Z. LIN. *Journal of Chemical Industry and Engineering (China)*, 2009, 3077-3081.
- 26 Z. Lu, C. X. Liu, X. Yu, Z. X. Lin. *Chinese Journal of Organic Chemistry*, 2013, **3**, 562-567.
- ⁷⁵ 27 X. Zhang, Y. Tian, Z. Li, X. Tian, H. Liu, H. Sun, A. Moore, C. Ran. *Journal of the American Chemical Society*, 2013.
- 28 I. Kheterpal, M. Chen, K. D. Cook, R. Wetzel. *Journal of molecular biology*, 2006, **4**, 785-795.
- ⁸⁰ 29 H. Levine-III, T. Thioflavine. *Protein Sci*, 1993, 404-410.
- 30 H. Liu, Z. Li, D. Qiu, Q. Gu, Q. Lei, L. Mao. *Neuroscience letters*, 2010, **2**, 83-88.
- 31 T. M. Bass, D. Weinkove, K. Houthoofd, D. Gems, L. Partridge. *Mechanisms of ageing and development*, 2007, **10**, 546-552.
- ⁸⁵ 32 S.-Y. Chen, Y. Chen, Y.-P. Li, S.-H. Chen, J.-H. Tan, T.-M. Ou, L.-Q. Gu, Z.-S. Huang. *Bioorganic & medicinal chemistry*, 2011, **18**, 5596-5604.